

Self-assembled nanotube field-effect transistors for label-free protein biosensors

P. Hu,¹ A. Fasoli,¹ J. Park,² Y. Choi,^{1,2} P. Estrela,¹ S. L. Maeng,² W. I. Milne,¹ and A. C. Ferrari^{1,a)}

¹*Department of Engineering, University of Cambridge, 9 J.J. Thomson Avenue, Cambridge CB3 0FA, United Kingdom*

²*Electronics and Telecommunications Research Institute, 161 Gajeong-dong, Yuseong-gu, Daejeon 305-350, Republic of Korea*

(Received 1 June 2008; accepted 9 August 2008; published online 6 October 2008)

A self-assembly method is developed to fabricate single-wall carbon nanotube field-effect transistors (SWNT-FETs). The electrode surface and the area between electrodes are modified with nonpolar groups ($-\text{CH}_3$) and polar groups ($-\text{NH}_3^+$). SWNTs are selectively placed in the area between the electrodes. We achieve stability and specificity in label-free protein detection using the biotin-streptavidin pair as research model. Our process holds promise for high integration of SWNT-FET biosensors, with no need for high-temperature processing. © 2008 American Institute of Physics. [DOI: 10.1063/1.2988274]

I. INTRODUCTION

Label-free biosensors with high miniaturization and integration have drawn intense interest since they could potentially make advanced molecular diagnostics available for low cost routine practice.^{1–7} Current sensing mainly focuses on optical detection using fluorescent-labeled biomolecules with dyes^{8–10} or quantum dots.^{11–13} Artificially labeled materials are time consuming and cost intensive,^{5,6} and the introduction of labels weakens the interaction between receptor and target.⁶ Hence, the development of fully electronic label-free sensing techniques is highly desirable.^{1–5}

The electrical conductance of a semiconducting single-wall carbon nanotube (SWNT) is sensitive to its environment and varies significantly with surface adsorption of various chemicals and biomolecules.^{14–19} This makes SWNT field-effect transistors (SWNT-FETs) very promising candidates for label-free biosensing.

Sensitivity is a key factor for a sensor, and reflects its minimum detectable concentration.²⁰ Recently reported nanotube biosensors have shown reliable high detection limits between 100 pM and 100 nM for proteins,^{18–20} and potential for large-scale arrayability.^{7,18–22} Indeed, the use of nanotube biosensor requires arrays of devices on wafers.^{20,22} It is thus essential to develop assembling techniques for mass production of SWNT-FETs on given substrates with control over SWNT location and orientation.

To date, the assembly and integration of SWNT-FETs is generally performed in two ways, *in situ* chemical vapor deposition (CVD)^{23–26} or postgrowth fabrication.^{27–37} So far, the lowest reported CVD growth temperature is 350 °C,²⁶ but *in situ* growth approaches for parallel assembly usually involve very high temperature (>700 °C).^{23–25} This limits their application in some pre-existing circuit structures. Alignment and selective deposition of as-grown SWNTs were demonstrated by using

surface-modified substrates,^{27–29} electric fields,^{30–35} and AFM manipulation,³⁶ but these approaches suffer from shortcomings, such as complex operation, or the need for special equipment. Therefore, it is still desirable to develop a method for selective incorporation of SWNTs into integrated circuits using a simple, low-cost, high-yield, self-assembly-based technique.

II. EXPERIMENTAL

We use High Pressure CO conversion (HiPCo) SWNT (from Carbon Nanotechnologies), biotin-N-hydroxylsuccinimide ester (biotin) and streptavidin (from Molecular Probes), bovine immunoglobulin (IgG) (from Sigma-Aldrich), poly(ethylene imine) (PEI) (average molecular weight of 25 000, Aldrich), and poly(ethylene glycol) (PEG) (average molecular weight of 1000, Aldrich).

Cr/Au electrode patterns are made using conventional UV lithography and lift-off on *n*-type silicon wafers with a 200 nm thermally oxidized layer. The electrodes are 10/100 (Cr/Au) nm, with a gap of 5–10 μm.

The surface of a wafer bearing electrode patterns is functionalized with nonpolar ($-\text{CH}_3$) or polar ($-\text{NH}_3^+$) groups in selected areas. The detailed procedure is as follows. The SiO₂ surface between gaps is hydroxylated in a solution of ammonium hydroxide/hydrogen peroxide/water (1:1:4), and terminated with an amino-group by immersing the wafer into 2% aminopropyltriethoxysilane (APTES) in 95% acetone for 1 h.³⁸ Subsequently, the surface of the gold electrodes is covered with a self-assembled monolayer of octanethiol by immersing the wafer in 2% methanol solution of octanethiol for 12 h. To selectively deposit SWNTs in the gap area, the functionalized wafer is immersed in a solution of SWNTs in 1,2-dichlorobenzene (~0.02 mg/ml) for 1 min. The SWNT solution of 1,2-dichlorobenzene is prepared by sonicating 0.2 mg SWNT in 10 ml 1,2-dichlorobenzene for 15 min. The device structure is checked by high-resolution scanning electron microscopy (SEM) (FEI Philips XL30 sFEG). The elec-

^{a)}Electronic mail: acf26@eng.cam.ac.uk.

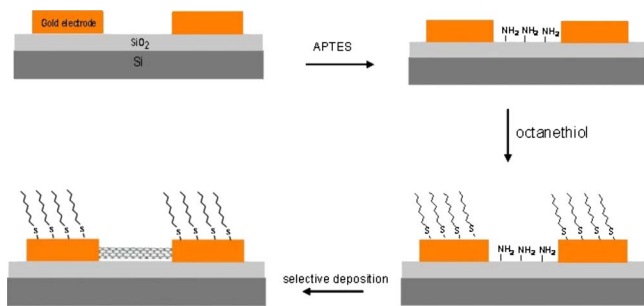


FIG. 1. (Color online) Scheme of the self-assembly procedure for SWNT-FET fabrication.

trical properties of SWNT-FETs without additional annealing in vacuum are measured using a Wentworth MP1008 probe station and a HP 4156A semiconductor parameter analyzer at ambient conditions.

The nanotubes in the device are coated with a layer of PEI and PEG. These polymers are used for covalent attachment of biomolecules and prohibition of physical adsorption of proteins.^{18,39} To do so, the device is submerged in 5% water solution of PEI and PEG for 12–18 h, followed by rinsing in de-ionized water for 1 h. The polymer-coated devices are biotinylated by immersing them in a 10 mM water solution of biotin-N-hydroxysuccinimide ester at room temperature for 2 h. Subsequently, the biotinylated polymer-coated devices are exposed to phosphate buffered saline (PBS) (0.02 M, pH 7.2) solution containing 50 nM of streptavidin at room temperature for 30 min. Then, the devices are rinsed with water and blown dry with nitrogen. To test the specificity of the biosensor, the device is exposed to 50 nM IgG in PBS buffer, which should not interact with the biotin layer. Then, real-time monitoring of the electronic signal is carried out.

III. RESULTS AND DISCUSSION

The self-assembly procedure for SWNT-FET fabrication is shown in Fig. 1. The surfaces of the gold electrodes and the area between electrodes are functionalized with nonpolar groups ($-\text{CH}_3$) and polar groups ($-\text{NH}_3^+$), respectively. X-ray photoelectron spectroscopy (XPS) is used to probe the effectiveness of this selective functionalization by determining the elemental composition of the surface. Nitrogen is present in the amino groups in APTES, but it is not in octanethiol. XPS data acquired in an area between electrodes shows the nitrogen 1s peak with a binding energy of 400 eV, indicating APTES functionalization.³⁸ No nitrogen peak is detected on the surface of the gold electrodes.

Previous studies show that SWNTs tend to deposit in areas covered with polar chemicals when the wafer is dipped in a SWNT solution.²⁷ By exploiting this, we develop a self-assembly approach for selective deposition of SWNT between electrodes. Figure 2(a) shows a low magnification SEM image of our integrated nanotube FET. Figure 2(b) presents the magnified image of the device, where SWNTs are deposited in the area between electrodes and contact the electrodes. The surface of the gold electrode is clean, show-

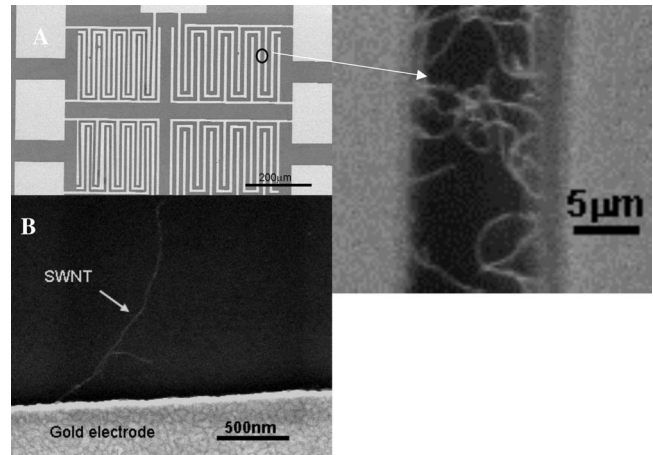


FIG. 2. SEM images of FET chip. Magnified images show SWNTs selectively deposited between electrodes, contacting source and drain. Note that the electrode surface is clean.

ing the effectiveness of our method. The SEM images clearly indicate that our devices are nanotube network transistors.

Present growth methods always produce a mixture of metallic SWNTs (m -SWNT) and semiconducting ones (s -SWNT). Removing m -SWNTs could allow us to better exploit the conductance changes in s -SWNT as a result of binding of biological macromolecules to the surface.^{14–18} Electrical breakdown (BD) is an effective way to eliminate m -SWNT in individual SWNT devices.^{40,41} This may not be the case in network SWNTs.⁴² One important difference between SWNT networks and individual SWNTs is that, in networks, intertube processes dominate^{42–46} and transport can be explained by the percolation theory.^{43–48} Total elimination of m -SWNTs in network devices is not strictly necessary for sensing applications. Network devices with high percentage ($>60\%$) of s -SWNTs can show field effect and be used for biosensing.¹⁸ However, even in network SWNT devices, voltage pulses can significantly increase the on/off ratio, whatever the microscopic mechanism, be it BD, oxidation, selective cutting, or incomplete m -SWNT removal. Thus, we do so here, by applying a high gate voltage ($V_G = 30$ V) to deplete s -SWNTs. Figures 3(a) and 3(b) show a comparison of the $I_{\text{DS}}-V_G$ characteristics of a representative device, before and after this procedure. The on/off ratio increases from less than 10 to about 10^4 .

The $I_{\text{DS}}-V_G$ characteristic ($V_{\text{DS}} = 1$ V) of a typical device is plotted in Fig. 4. It shows high conductance ($>10^{-6}$ A) under negative gate bias and almost none ($\sim 10^{-10}$ A) for positive gate bias. The device turns on with an on-off ratio of approximately 3×10^4 . The drain current decreases as V_G goes from -15 to -3.5 V. Almost no conduction is seen from -3.5 V to higher positive gate biases. This indicates that the carriers are holes and the device behaves as p -type. Previous works attributed this p -type behavior to adsorbed O_2 from the ambient.^{15,16,49,50}

The threshold voltage V_{th} (the gate voltage for which the device starts to turn on) is approximately -3.5 V. The subthreshold swing, defined as $S = dV_G/d \log(I_{\text{DS}})$, is a key parameter to transistor miniaturization.⁵⁰ A small S is desired for low threshold voltage and low-power operation in FETs

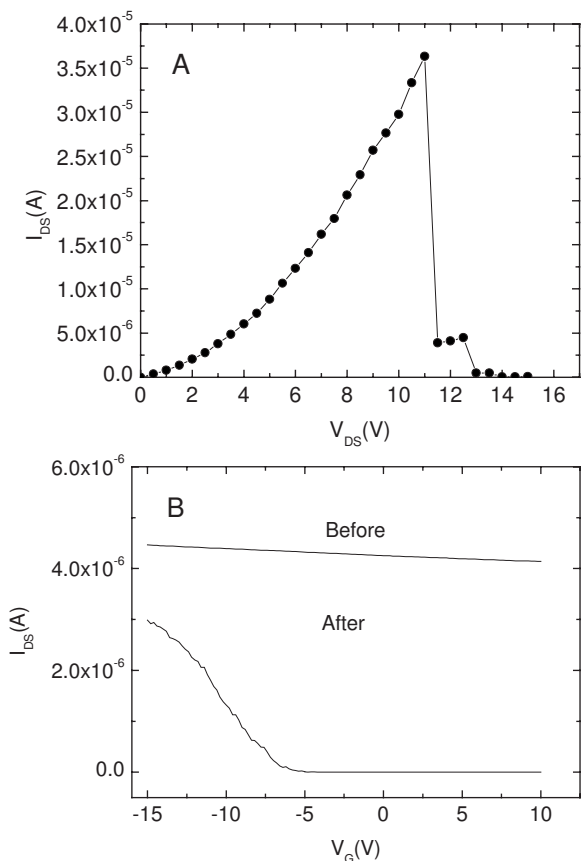


FIG. 3. (a) Change in I_{DS} - V_{DS} characteristic of SWNT-FET caused by a current pulse at $V_G=30$ V. (b) Comparison of I_{DS} - V_G characteristics of a typical SWNT-FET device before and after the procedure show in (a), at $V_{DS}=1$ V. On/off ratio increases from 10 to 10^4 .

scaled down to small sizes. We extract subthreshold swings for all our p -type SWNT FETs in the range of 300 ± 100 mV per decade, similar to previous results for individual SWNT-FETs (Refs. 16 and 49–54). In addition, our self-assembled SWNT network transistors show a minimal hysteresis.⁵⁵

Figure 5 shows the architecture of our nanotube biosensor. Coating polymers (PEI and PEG) on SWNT is a noncovalent functionalization method.^{18,41,56} The amino groups in PEI covalently attach receptor molecules to the nanotube sur-

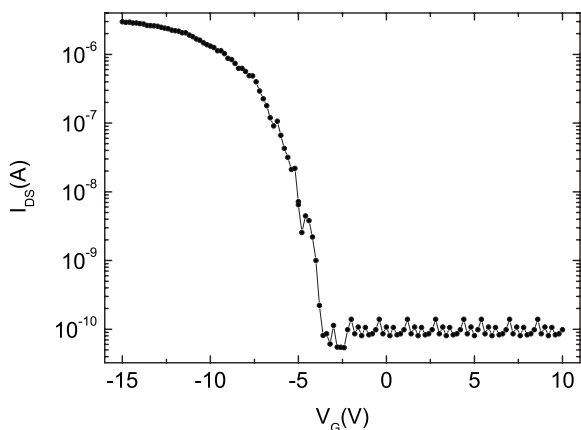


FIG. 4. I_{DS} - V_G characteristic at $V_{DS}=1$ V of a typical device, behaving as a p -type FET. On/off ratio is about 3×10^4 .

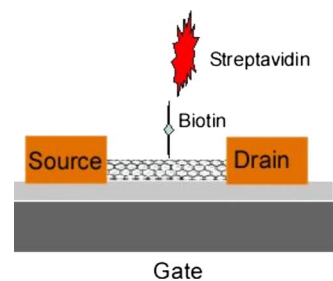


FIG. 5. (Color online) Schematic of the nanotube FET biosensor. Nanotubes are functionalized with a molecular receptor, biotin. The target protein is streptavidin.

face. Polymer coating can efficiently prohibit nonspecific adsorption of biomolecules. PEI and PEG are thus used to avoid the physical absorption of proteins on the nanotube surface.^{39,53} In order to remove PEI and PEG nonspecifically adsorbed on the nanotube surface, the device is rinsed in water.¹⁵

We exploit the biotin-streptavidin pair to demonstrate the effectiveness of the device architecture. It is known that biotin binds to streptavidin specifically.⁵⁷ The electrical properties of the SWNT-FETs are measured in real time at room temperature. We measure (1) the bare nanotube FET, (2) nanotube FET with PEI and PEG coating, (3) nanotube FET with biotin attachment, and (4) nanotube FET with streptavidin binding. The change in the device characteristic after steps 1–4 is shown in Fig. 6. This plots the drain current-drain bias characteristics at $V_G=-5$ V before and after every modification on the SWNT channel. As shown in Fig. 6(a),

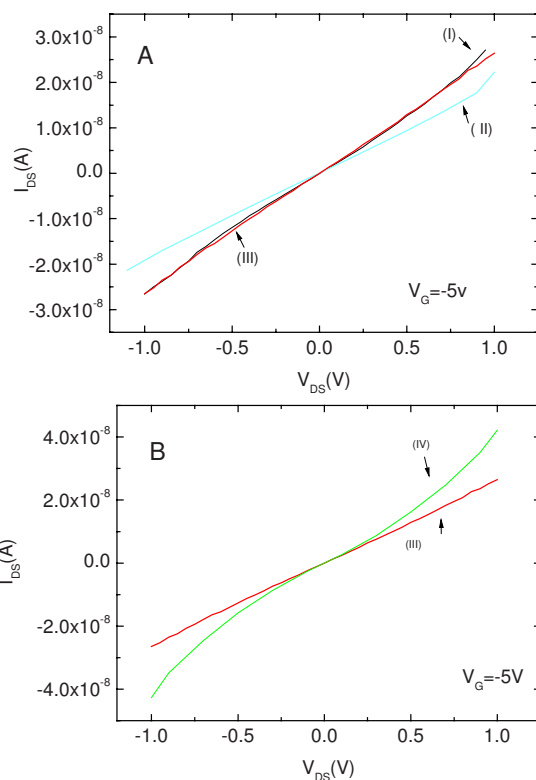


FIG. 6. (Color online) I_{DS} - V_{DS} characteristics of the SWNT-FET $V_G=-5$ V for: (I) bare SWNT-FET, (II) PEI coated SWNT-FET, (III) biotinylated SWNT-FET, and (IV) after streptavidin binding.

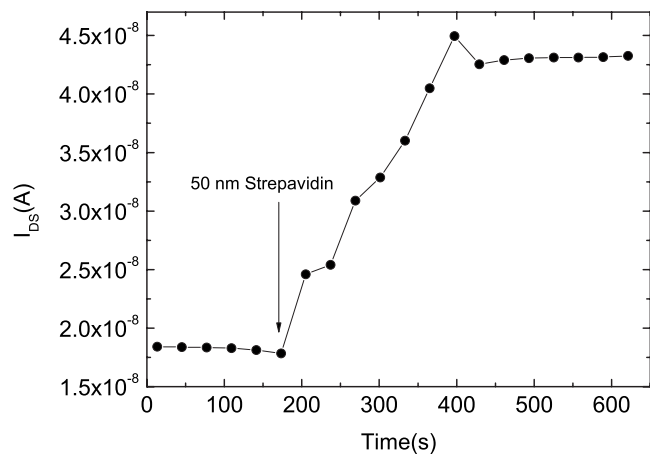


FIG. 7. Time dependence of the SWNT-FET I_{DS} at $V_{DS}=0.2$ V and $V_G=-5$ V after the introduction of target streptavidin onto the biotinylated SWNT-FET. The arrow indicates the time of streptavidin addition.

the PEI coated SWNT-FET (curve II) has lower conductance compared to the bare one (curve I). This decrease in conductance can be assigned to partial depletion of holes in the p -type SWNT-FET by electron donation from the amine groups in the polymer.¹⁷ Amino groups are converted into amide groups by reaction with the biotin-N-hydroxylsuccinimide ester. Amide groups cannot act as electron donor, so the conductance of biotinylated FET (curve III) recovers to the level of the bare FET. This indicates that biotin is successfully covalently attached to the SWNT channels. Curve IV in Fig. 6(b) shows a sharp increase in conductance after the biotinylated FET is exposed to the target streptavidin (50 nM), indicating that the target is detected successfully.

We also monitor real-time detection. Figure 7 shows the time dependence of I_{DS} at $V_{DS}=0.2$ V and at $V_G=-5$ V after the introduction of target streptavidin (50 nM) onto the biotinylated device. Adding the target streptavidin causes a sharp increase in the source-drain current and then a gradual saturation at slightly lower values.

The increase in conductance upon addition of streptavidin is consistent with binding of a negatively charged species to the surface of a p -type SWNT, and streptavidin (isoelectronic point (pI): ~ 5 to 6) being negatively charged at the pH of our measurements ($pH=7.2$).⁵⁷ Therefore, our results indicate that streptavidin is successfully bound to the SWNT channels via biological recognition of the biotin-streptavidin pair.

Complete coating of PEG is crucial for suppression of physical binding and, thus, improvement of selectivity and specificity of the sensor. Therefore, the devices are treated in a PEG solution for at least 12 h. Control experiments are then carried out in order to investigate the stability and specificity of our biosensors. Figure 8 shows the time dependence of the SWNT-FET responses at $V_{DS}=0.2$ V and $V_G=-5$ V. No significant conductance change is observed after exposure to the blank PBS. The specificity of the biosensor is tested by applying the control protein IgG. When the biosensor is exposed to IgG (50 nM), no significant I_{DS} change is observed (Fig. 8). This shows that the biosensor only re-

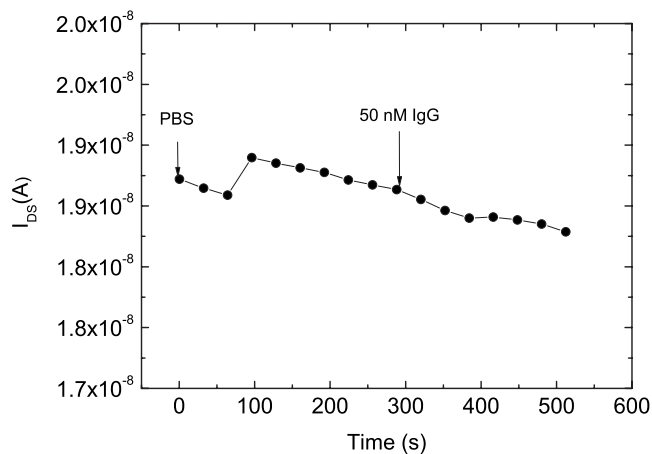


FIG. 8. Time dependence of the SWNT-FET I_{DS} at $V_{DS}=0.2$ V and $V_G=-5$ V after the introduction of a blank buffer (PBS) solution and non-target IgG onto the biotinylated SWNT-FET. Arrows indicate the time of PBS and IgG addition, respectively.

sponds to the detection target (streptavidin) and thus is specific and highly selective. In addition, this also indicates that nonspecific binding of IgG is successfully suppressed by the PEI and PEG coatings.

IV. CONCLUSIONS

We demonstrated SWNT-FETs fabricated via a selective functionalization approach. The SWNTs are selectively deposited in an APTES modified area between electrodes. We discussed their sensing applications using biotin-streptavidin as research model, and demonstrated high stability and specificity. This fabrication method can be extended for large-scale assembly of SWNT-FETs, without any high-temperature processing, and can be ideal for high integration of SWNT-FET biosensors.

ACKNOWLEDGMENTS

This work is supported by the Ministry of Information and Communication, Republic of Korea, under Grant No. A1100-0602-0101. ACF acknowledges funding from The Royal Society and The Leverhulme Trust.

¹B. R. Baker, R. Y. Lai, M. S. Wood, E. H. Doctor, A. J. Heeger, and K. W. Plaxco, *J. Am. Chem. Soc.* **128**, 3138 (2006).

²Z. Q. Gao, A. Agarwal, A. D. Trigg, N. Singh, C. Fang, C. H. Tung, Y. Fan, K. D. Buddharaju, and J. M. Kong, *Anal. Chem.* **79**, 3291 (2007).

³Y. Cui, Q. Q. Wei, H. K. Park, and C. M. Lieber, *Science* **293**, 1289 (2001).

⁴G. F. Zheng, F. Patolsky, Y. Cui, W. U. Wang, and C. M. Lieber, *Nat. Biotechnol.* **23**, 1294 (2005).

⁵J. H. Lu, C. M. Strohsahl, B. L. Miller, and L. J. Rothberg, *Anal. Chem.* **76**, 4416 (2004).

⁶B. L. Li, H. Wei, and S. J. Dong, *Chem. Commun. (Cambridge)* **2007**, 73.

⁷A. Star, E. Tu, J. Niemann, J. C. P. Gabriel, C. S. Joiner, and C. Valcke, *Proc. Natl. Acad. Sci. U.S.A.* **103**, 921 (2006).

⁸B. N. G. Giepmans, S. R. Adams, M. H. Ellisman, and R. Y. Tsien, *Science* **312**, 217 (2006).

⁹C. J. Weijer, *Science* **300**, 96 (2003).

¹⁰A. C. Pease, D. Solas, E. J. Sullivan, M. T. Cronin, C. P. Holmes, and S. P. A. Fodor, *Proc. Natl. Acad. Sci. U.S.A.* **91**, 5022 (1994).

¹¹C. C. Huang and H. T. Chang, *Anal. Chem.* **78**, 8332 (2006).

¹²J. K. Herr, J. E. Smith, C. D. Medley, D. H. Shangguan, and W. H. Tan, *Anal. Chem.* **78**, 2918 (2006).

- ¹³D. Gerion, F. Q. Chen, B. Kannan, A. H. Fu, W. J. Parak, D. J. Chen, A. Majumdar, and A. P. Alivisatos, *Anal. Chem.* **75**, 4766 (2003).
- ¹⁴J. C. Charlier, X. Blasé, and S. Roche, *Rev. Mod. Phys.* **79**, 677 (2007).
- ¹⁵J. Kong, N. R. Franklin, C. W. Zhou, M. G. Chapline, S. Peng, K. J. Cho, and H. J. Dai, *Science* **287**, 622 (2000).
- ¹⁶P. G. Collins, K. Bradley, M. Ishigami, and A. Zettl, *Science* **287**, 1801 (2000).
- ¹⁷M. Shim, A. Javey, N. W. S. Kam, and H. J. Dai, *J. Am. Chem. Soc.* **123**, 11512 (2001).
- ¹⁸R. J. Chen, S. Bangsaruntip, K. A. Drouvalakis, N. W. S. Kam, M. Shim, Y. M. Li, W. Kim, P. J. Utz, and H. J. Dai, *Proc. Natl. Acad. Sci. U.S.A.* **100**, 4984 (2003).
- ¹⁹H. R. Byon and H. C. Choi, *J. Am. Chem. Soc.* **128**, 2188 (2006).
- ²⁰S. Sotiropoulou and N. A. Chaniotakis, *Anal. Bioanal. Chem.* **375**, 103 (2003).
- ²¹Q. F. Pengfei, O. Vermesh, M. Grecu, A. Javey, O. Wang, H. J. Dai, S. Peng, and K. J. Cho, *Nano Lett.* **3**, 347 (2003).
- ²²B. Mahar, C. Laslau, R. Yip, and Y. Sun, *IEEE Sens. J.* **7**, 266 (2007).
- ²³Y. G. Zhang, A. L. Chang, J. Cao, Q. Wang, W. Kim, Y. M. Li, N. Morris, E. Yenilmez, J. Kong, and H. J. Dai, *Appl. Phys. Lett.* **79**, 3155 (2001).
- ²⁴N. R. Franklin and H. J. Dai, *Adv. Mater. (Weinheim, Ger.)* **12**, 890 (2000).
- ²⁵S. M. Huang, M. Woodson, R. Smalley, and J. Liu, *Nano Lett.* **4**, 1025 (2004).
- ²⁶M. Cantoro, S. Hofmann, S. Pisana, V. Scardaci, A. Parvez, C. Ducati, A. C. Ferrari, A. M. Blackburn, K. Y. Wang, and J. Robertson, *Nano Lett.* **6**, 1107 (2006).
- ²⁷J. Liu, M. J. Casavant, M. Cox, D. A. Walters, P. Boul, W. Lu, A. J. Rimberg, K. A. Smith, D. T. Colbert, and R. E. Smalley, *Chem. Phys. Lett.* **303**, 125 (1999).
- ²⁸S. G. Rao, L. Huang, W. Setyawan, and S. H. Hong, *Nature (London)* **425**, 36 (2003).
- ²⁹J. X. Yu, J. G. Shapter, J. S. Quinton, M. R. Johnston, and D. A. Beattie, *Phys. Chem. Chem. Phys.* **9**, 510 (2007).
- ³⁰Z. Chen, Y. L. Yang, F. Chen, Q. Qing, Z. Y. Wu, and Z. F. Liu, *J. Phys. Chem. B* **109**, 11420 (2005).
- ³¹L. A. Nagahara, I. Amlani, J. Lewenstein, and R. K. Tsui, *Appl. Phys. Lett.* **80**, 3826 (2002).
- ³²X. Q. Chen, T. Saito, H. Yamada, and K. Matsushige, *Appl. Phys. Lett.* **78**, 3714 (2001).
- ³³L. F. Dong, V. Chirayos, J. Bush, J. Jiao, V. M. Dubin, R. V. Chebrian, Y. Ono, J. F. Conley, and B. D. Ulrich, *J. Phys. Chem. B* **109**, 13148 (2005).
- ³⁴S. Banerjee, B. E. White, L. M. Huang, B. J. Rego, S. O'Brien, and I. P. Herman, *J. Vac. Sci. Technol. B* **24**, 3173 (2006).
- ³⁵A. Vijayaraghavan, S. Blatt, D. Weissenberger, M. Oron-Carl, F. Henrich, D. Gerthsen, H. Hahn, and R. Krupke, *Nano Lett.* **7**, 1556 (2007).
- ³⁶J. Lefebvre, J. F. Lynch, M. Llaguno, M. Radosavljevic, and A. T. Johnson, *Appl. Phys. Lett.* **75**, 3014 (1999).
- ³⁷X. L. Li, L. Zhang, X. R. Wang, I. Shimoyama, X. M. Sun, W. S. Seo, and H. J. Dai, *J. Am. Chem. Soc.* **129**, 4890 (2007).
- ³⁸G. J. Zhang, T. Tani, T. Zako, T. Funatsu, and I. Ohdomari, *Sens. Actuators B* **97**, 243 (2004).
- ³⁹M. Shim, N. W. S. Kam, R. J. Chen, Y. M. Li, and H. J. Dai, *Nano Lett.* **2**, 285 (2002).
- ⁴⁰P. C. Collins, M. S. Arnold, and P. Avouris, *Science* **292**, 706 (2001).
- ⁴¹M. Lazzeri, S. Piscanec, F. Mauri, A. C. Ferrari, and J. Robertson, *Phys. Rev. Lett.* **95**, 236802 (2005).
- ⁴²G. Fanchini, H. E. Unalan, and M. Chhowalla, *Nano Lett.* **7**, 1129 (2007).
- ⁴³S. Kumar, J. Y. Murthy, and M. A. Alam, *Phys. Rev. Lett.* **95**, 066802 (2005).
- ⁴⁴S. Kumar, J. Y. Murthy, and M. A. Alam, *Appl. Phys. Lett.* **88**, 123505 (2006).
- ⁴⁵N. Pimparkar, Q. Cao, S. Kumar, J. Y. Murthy, J. Rogers, and M. A. Alam, *IEEE Electron Device Lett.* **28**, 157 (2007).
- ⁴⁶Y. Zhou, A. Gaur, S.-H. Hur, C. Kocabas, M. A. Meitl, M. Shim, and J. A. Rogers, *Nano Lett.* **4**, 2031 (2004).
- ⁴⁷N. Pimparkar, Q. Cao, S. Kumar, J. Y. Murthy, J. Rogers, and M. A. Alam, *IEEE Electron Device Lett.* **28**, 2 (2007).
- ⁴⁸Q. Cao, H. S. Kim, N. Pimparkar, J. P. Kulkarni, C. Wang, M. Shim, K. Roy, M. A. Alam, and J. A. Rogers, *Nature (London)* **454**, 495 (2008).
- ⁴⁹S. J. Tans, A. R. M. Verschueren, and C. Dekker, *Nature (London)* **393**, 49 (1998).
- ⁵⁰S. H. Jhi, S. G. Louie, and M. L. Cohen, *Phys. Rev. Lett.* **85**, 1710 (2000).
- ⁵¹C. G. Lu, Q. Fu, S. M. Huang, and J. Liu, *Nano Lett.* **4**, 623 (2004).
- ⁵²A. Javey, H. Kim, M. Brink, Q. Wang, A. Ural, J. Guo, P. McIntyre, P. McEuen, M. Lundstrom, and H. J. Dai, *Nat. Mater.* **1**, 241 (2002).
- ⁵³S. Auvray, V. Derycke, M. Goffman, A. Filoramo, O. Jost, and J. P. Bourgoin, *Nano Lett.* **5**, 451 (2005).
- ⁵⁴X. L. Li, Y. Q. Liu, D. C. Shi, Y. M. Sun, G. Yu, D. B. Zhu, H. M. Liu, X. Y. Liu, and D. X. Wu, *Appl. Phys. Lett.* **87**, 243102 (2005).
- ⁵⁵P. Hu, C. Zhang, A. Fasoli, V. Scardaci, S. Pisana, T. Hasan, J. Robertson, W. I. Milne, and A. C. Ferrari, *Physica E (Amsterdam)* **40**, 2278 (2008).
- ⁵⁶S. Vajda, Z. P. Weng, R. Rosenfeld, and C. Delisi, *Biochemistry* **33**, 13977 (1994).
- ⁵⁷E. A. Bayer and M. Wilchek, *Methods Enzymol.* **184**, 49 (1990).